Journal of Chromatography A, 1236 (2012) 177–188

Contents lists available at SciVerse ScienceDirect

Journal of Chromatography A

journal homepage: www.elsevier.com/locate/chroma

Evaluation of a new wide pore core–shell material (Aeris™ WIDEPORE) and comparison with other existing stationary phases for the analysis of intact proteins

Szabolcs Fekete[a,*], Róbert Berky[b,1], Jenő Fekete[b,1], Jean-Luc Veuthey[a,2], Davy Guillarme[a,2]

[a] School of Pharmaceutical Sciences, University of Geneva, University of Lausanne, Bd d'Yvoy 20, 1211 Geneva 4, Switzerland
[b] Budapest University of Technology and Economics, Department of Inorganic and Analytical Chemistry, Szt. Gellért tér 4., 1111 Budapest, Hungary

ARTICLE INFO

Article history:
Received 11 November 2011
Received in revised form 2 March 2012
Accepted 6 March 2012
Available online 10 March 2012

Keywords:
Column efficiency
Peak capacity
Protein separation
Core–shell
Aeris WIDEPORE
Monoclonal antibody

ABSTRACT

The separation of large biomolecules such as proteins or monoclonal antibodies (mAbs) by RPLC can be drastically enhanced thanks to the use of columns packed with wide-pore porous sub-2 μm particles or shell particles. In this context, a new wide-pore core–shell material has been recently released under the trademark Aeris WIDEPORE. It is made of a 3.2 μm solid inner core surrounded by a 0.2 μm porous layer (total particle size of 3.6 μm). The aim of this study was to evaluate the performance of this new material, compare it to other recently developed and older conventional wide-pore columns and demonstrate its applicability to real-life separations of proteins and mAbs. At first, the traditional h_{min} values of the Aeris WIDEPORE column were determined for small model compounds. The h_{min} values were equal to 1.7–1.8 and 1.4 for the 2.1 and 4.6 mm I.D. columns, respectively, which are in agreement with the values reported for other core–shell materials. In the case of a small protein Insulin (5.7 kDa), the achievable lowest *h* value was below 2 and this impressive result confirms that the Aeris WIDEPORE material should be dedicated to protein analysis. This column was then compared with five other commercially available wide-pore and medium-pore stationary phases, in the gradient elution mode, using various flow rates, gradient steepness and model proteins of MW = 5.7–66.8 kDa. The Aeris WIDEPORE material often provided the best performance, in terms of peak capacity, peak capacity per time and pressure unit (PPT) and also based on the gradient kinetic plot representation. Finally, real separations of filgrastim (18.8 kDa) and its oxidized and reduced forms were performed on the different columns and the Aeris WIDEPORE material provided the most impressive performance (peak capacity > 100 for t_{grad} < 6 min). Last but not least, this new material was also evaluated on digested and reduced mAb and powerful, high-throughput separations were also attained.

1. Introduction

Columns of sub-3 μm superficially porous particles (also known as core–shell, fused-core or porous shell particles) recently have had significant impact on the liquid chromatographic separation of small molecules. The success of columns packed with these particles is mostly based on their comparable efficiency to that of columns made with sub-2 μm fully porous particles, but at about one-half operating pressure [1–6]. Superficially porous particles manifest the advantages of porous and some benefit of nonporous particles. Several types of the new generation of superficially porous materials are now commercially available (5 μm, 2.7 μm, 2.6 μm and 1.7 μm) [7]. The kinetic efficiency of columns packed with these shell particles is improved when the porous shell thickness is decreased. However, the optimum shell thickness in reality is likely to be a compromise between efficiency, sample loading capacity and analyte retention. Now it seems that the structure of the last generation of shell-particles is very close to its optimum in terms of the column efficiency and loadability.

Recent development and commercialization of the latest generation of core–shell columns have not included media with pore sizes of around 300 Å, which are regarded essential for macromolecule separations. However, a 160 Å packing was introduced in 2010 by Advanced Material Technology (AMT) and Sigma–Aldrich under the brand names of Halo Peptide ES-C18 and Ascentis Express Peptide ES-C18, respectively [8,9]. These particles have the same physical dimensions as the Halo or Ascentis Express particles

* Corresponding author. Tel.: +36 30 395 6657.
E-mail addresses: szfekete@mail.bme.hu, szabolcs.fekete@unige.ch (S. Fekete), berkinator@gmail.com (R. Berky), fekete@mail.bme.hu (J. Fekete), Jean-Luc.Veuthey@unige.ch (J.-L. Veuthey), davy.guillarme@unige.ch (D. Guillarme).
[1] Tel.: +36 30 395 6657.
[2] Tel.: +41 22 379 6334.

0021-9673/$ – see front matter © 2012 Elsevier B.V. All rights reserved.
doi:10.1016/j.chroma.2012.03.018

applied for small molecule analyses, but with a larger average pore size of about 160 Å allowing for the unrestricted access of molecules up to about 15,000 Da, depending on the molecular conformation [10]. In a recent study, Kirkland et al. compared the efficiency performance of the 160 Å Halo Peptide ES-C18 column to the original 90 Å Halo-C18 column for mixtures of peptides and small proteins [8]. The smaller peptides eluted with equivalent efficiency from both columns. However the small proteins (i.e. ribonuclease, insulin, cytochrome c and lysozyme) with MW ranging between 5.7 and 14.6 kDa showed broadened peaks on the 90 Å Halo-C18 column, indicating restricted diffusion, but narrow peaks on the 160 Å Halo Peptide ES-C18 column. Gritti and Guiochon also investigated the performance of the new 160 Å Halo Peptide ES material [9]. Their results confirmed that the Halo Peptide ES column, designed to resolve mixtures of large molecules, provided markedly better kinetic performance than the first generation of Halo particles did. The physico-chemical explanations for these observations might not necessarily be those anticipated during the design of this new packing material. Indeed, the initial incentive was to increase the mesopore size in order to reduce the hindrance to diffusion through the porous shells of the particles. Successfully enough, the sample diffusivity in the porous shells was increased. However, their results also proved that the trans-particle mass transfer resistance term is not the limiting kinetic factor that controls the solid–liquid mass transfer resistance in Halo particles. According to Gritti and Guiochon, the van Deemter *C* term (associated with mass transfer resistance) of large molecules is mostly accounted for by a slow external film mass transfer [9]. It seems that the improvement in the column efficiency for large molecules could be related to the easier access of their molecules to the internal volume. The improvement in column performance is also due to the reduced eddy dispersion term (*A* term) of the Halo Peptide ES 160 Å column, which is 25% smaller than that of the first generation of Halo 90 Å column (as for small analytes). This diminution of the *A* term emphasizes the important role of sample diffusivity through particles in the relaxation of radial concentration gradients caused by short-range inter-channel and trans-column velocity biases [9]. Now, a 3.6 μm core–shell material has been recently launched by Phenomenex under the name of Aeris WIDEPORE. As an alternative to core–shell particles, columns packed with wide pore sub-2 μm fully porous particles are commercially available (Waters Acquity BEH300) and showed excellent performance in peptide and protein separations [11].

The aim of this study was to perform a critical evaluation of the practical possibilities and limitations of this new commercially available wide pore core–shell material. Isocratic measurements were performed with small molecular weight test analytes (estradiol and ivermectin) and with insulin in order to assess the achievable reduced plate height minimum values of this new column. Two column dimensions (2.1 mm and 4.6 mm I.D.) were compared in terms of isocratic column efficiency.

The kinetic performance of this new column was also investigated and compared in gradient elution mode. Peak capacities of six 150 mm × 2.1 mm columns (all C18 stationary phases), packed with conventional 5 and 3 μm wide pore (300 Å) fully porous, sub-2 μm wide pore (300 Å) and intermediate pore size (175 Å) fully porous, 2.7 μm 160 Å and 3.6 μm wide pore superficially porous particles were obtained and investigated for protein separations. Intact proteins (5.7–66.8 kDa) and monoclonal antibody fragments (10–50 kDa) were separated in gradient mode at elevated temperature (T = 50 °C and 75 °C). The effect of flow rate and gradient time on the peak capacity and achievable separation time was studied and the potential of the six columns in protein separation was compared. Peak capacity plots, peak capacity per time unit and pressure unit plots as well as gradient kinetic plots were obtained and compared. Finally, some practical real-life examples are also shown, and present the potential of the new wide pore superficially porous packing for protein separation.

2. Experimental

2.1. Chemicals, columns

Acetonitrile and methanol (gradient grade) were purchased from Sigma–Aldrich. Water was obtained with a Milli-Q Purification System from Millipore (Bedford, MA, USA). Relatively small MW neutral analytes as real-life pharmaceutical compounds, model proteins and an IgG1 monoclonal antibody (and its fragments) were used as test probes. Estradiol (estra-1,3,5(10)-triene-3,17-diol, MW = 272 g/mol), was purchased from Sigma–Aldrich (Budapest, Hungary). Ivermectin (22,23-dihydroavermectin B1a, MW = 875 g/mol) was purchased from Bioastralis (Smitfield, Australia). All of the test proteins such as insulin (from bovine pancreas, MW ~ 5.7 kDa), cytochrome-c (from horse heart, MW ~ 12.4 kDa) myoglobin (from equine skeletal muscle, MW ~ 17.7 kDa) and bovine serum albumin (BSA, MW ~ 66.8 kDa) were purchased from Sigma–Aldrich (Buchs, Switzerland). Recombinant human granulocyte-colony stimulating factor (G-CSF or filgrastim, MW ~ 18.8 kDa) was obtained from Amgen (Switzerland). IgG monoclonal antibody (MW ~ 150 kDa) was purchased from Roche (Roche Pharma, Switzerland). For fragmenting the monoclonal antibody, dithiothreitol (DTT) and papain (from Carica papaya) were obtained from Sigma–Aldrich (Buchs, Switzerland). Trifluoroacetic acid (TFA), 30% hydrogen peroxide and methionine were purchased from Sigma–Aldrich (Buchs, Switzerland).

An Agilent Zorbax 300SB-C18 5 μm (150 mm × 2.1 mm) column was obtained from Agilent Technologies (Santa Clara, CA, USA). A Phenomenex Jupiter 3 μm C18 300 Å (150 mm × 2.0 mm) column was purchased from Phenomenex Inc (Torrance, CA, USA). An Acquity BEH-300 C18 column with a particle size of 1.7 μm (150 mm × 2.1 mm, 300 Å) was purchased from Waters (Milford, MA, USA). Hypersil Gold C18 column with a particle size of 1.9 μm (150 mm × 2.1 mm, 175 Å) was a gift from Thermo (Runcorn, UK). Ascentis Express Peptide ES C18 column (150 mm × 2.1 mm, 160 Å) was purchased from Sigma–Aldrich. The new Aeris WIDEPORE C18 columns packed with 3.6 μm core–shell particles (150 mm × 2.1 mm and 150 mm × 4.6 mm, 300 Å) were generous gift from Phenomenex Inc (Torrance, CA, USA).

2.2. Equipment, software

All measurements were performed using a Waters Acquity UPLC™ system equipped with a binary solvent delivery pump, an autosampler and an UV detector. The Waters Acquity system includes a 5 μL sample loop and a 0.5 μL flow-cell. The loop is directly connected to the injection switching valve (there is no needle seat capillary). The connection tube between the injector and column inlet was 0.13 mm I.D. and 250 mm long (passive preheating included), and the capillary located between the column and detector was 0.10 mm I.D. and 150 mm long. The overall extra-column volume (V_{ext}) is about 13 μL as measured from the injection seat of the auto-sampler to the detector cell. The measured dwell volume is 100 μL. The extra-column variance of the system was measured by injecting one of the small test analytes (estradiol) with a zero-dead-volume connector instead of the column at each flow rate and in the same mobile phase [12]. The extra-column peak dispersion (σ^2_{ec}) was determined in μL^2 according to both the half height and moment method [12]. The plate height values obtained with half-height and moment method were slightly different because of the asymmetrical peak shapes obtained in the absence of a column. The average extra-column peak variance of

our system was found to be around $\sigma^2_{ec} \sim 5 - 6\ \mu L^2$. Data acquisition and instrument control was performed by Empower Pro 2 Software (Waters).

Calculation and data transferring to obtain h–ν (reduced plate height versus reduced linear velocity), peak capacity and kinetic plots was achieved by using a home made Excel template. The least square non-linear curve fitting the experimental data was performed using the solver function of MS Excel.

2.3. Apparatus and methodology

2.3.1. Sample preparation and mobile phase composition

The isocratic mobile phase consisted of 80/20 (v/v%) water/acetonitrile for estradiol and 25/75 (v/v%) water/acetonitrile for ivermectin. For measuring the isocratic column efficiency for a large analyte (insulin) a mixture of water (0.1% TFA)/acetonitrile (0.1% TFA) 70/30 (v/v%) and 71/29 (v/v%) were used as mobile phase (at 50 °C and 35 °C, respectively) for the Aeris WIDEPORE standard bore (150 mm × 4.6 mm) column while the mobile phase compositions were 69/31 and 71/29 (v/v%) for the narrow bore (150 mm × 2.1 mm) column (at 50 °C and 35 °C, respectively). For the gradient separation of proteins the mobile phase "A" was 0.1% TFA in water while the mobile phase "B" was 0.1% TFA in acetonitrile.

The stock solutions of estradiol and ivermectin were prepared in methanol (1000 μg/ml). The solutions for the chromatographic runs were diluted from the stock solutions with the mobile phase. The final concentration of the test solutions was 10 μg/ml. The stock solution of insulin was made in water (10,000 μg/ml). The injected solutions were diluted with water (100 μg/ml).

The stock solutions of model proteins were prepared in water (1000 μg/ml) except insulin which was dissolved in 80/20 (v/v%) water/acetonitrile (0.1% TFA) solvent. The stock solutions were sonicated for 0.5 min in ultrasonic bath then homogenized (for 5 s with vortex mixer). After that, aliquots of stock solutions of each solute were transferred into low volume insert of sample vial and diluted to 100 μg/ml with water.

The intact filgrastim was directly injected as received (Neupogen concentrated solution 0.3 mg/ml). Reduced and oxidized protein samples were prepared to evaluate the performance of the Aeris WIDEPORE column in real-life protein separations. The intramolecular disulphide bonds of filgrastim were reduced by adding a small amount of dithiothreitol (DTT) to its solution and incubating at 30 °C for 60 min. The oxidation of methionine residues with hydrogen peroxide was relatively fast in the case of this protein. Oxidation of methionine residues results in alterations of the protein structure that affect the apparent molecular size and polarity, thus oxidized forms should be separated from the native molecule. The oxidation was performed by adding 2% (v/v) hydrogen peroxide (30%) to the protein solution, and after a 3 h long incubation time (at 30 °C) the oxidation was stopped by adding 0.5 mg methionine to the solution.

The IgG monoclonal antibody also has intramolecular disulfide bonds which were reduced with DTT. 0.05 mg of DDT was added to 100 μL protein solution (10 mg/ml) then it was incubated at 30 °C for 60 min. The protein was completely converted to the light chain and heavy chain components of the antibody.

Papain is a thiol protease that cleaves IgG antibodies at the heavy chain hinge region into three fragments, one Fc and two identical Fab fragments [13–15]. The digestion of the IgG antibody was initiated by the addition of papain (diluted to 100 μg/ml with water) to give a final protein:enzyme ratio of 100:1 (m/m%), the final digestion volume was 200 μL (in low volume insert of sample vial) [13]. The digestion was carried out at 40 °C for 2.5 h. After the digestion a small amount of DTT was added to the solution and incubated at 30 °C for 60 min to create reduced fragments of 10–25 kDa.

2.3.2. Evaluating the column efficiency

At first, the efficiency of standard (4.6 mm I.D.) and narrow bore (2.1 mm I.D.) Aeris WIDEPORE 150 mm long columns were investigated by constructing their Knox plots and by estimating their reduced plate height minimum values (h_{min}) [16]. The following equations were used for the calculations:

$$h = A\nu^{1/3} + \frac{B}{\nu} + C\nu \quad (1)$$

$$h = \frac{H}{d_p} \quad (2)$$

$$\nu = \frac{ud_p}{D_M} \quad (3)$$

where H is the theoretical plate height, d_p the particle size of the column packing material, u the chromatographic linear velocity of the mobile phase, D_M the analyte diffusion coefficient and A–C are constants accounting for band broadening. The A coefficient represents the eddy dispersion, the B term the longitudinal diffusion and the C parameter is related to mass transfer resistances. The analyte diffusion coefficients of estradiol and ivermectin were calculated with the Wilke–Chang equation [17], and the diffusion coefficient of insulin was taken from literature [9].

A small volume (1 μL) of different molecular weight compounds such as estradiol, ivermectin and insulin was injected during the flow study. Estradiol was eluted with water/acetonitrile 80/20 (v/v), ivermectin was eluted with water/acetonitrile 25/75 (v/v), and insulin was eluted with water (0.1% TFA)/acetonitrile (0.1% TFA) 69/31, 70/30 and 71/29 (v/v). The column temperature was set to 35 °C for all three analytes, except that insulin was also tested at 50 °C.

Three consecutive injections were performed at each flow rate and the average peak width was used for further calculation. The measured plate height values were corrected for extra column band broadening.

Real-life protein separations are carried out in gradient elution mode at elevated temperatures. Since our purpose was to study the column performance under real conditions, gradient protein separations were performed under various conditions to evaluate the performance of the new Aeris WIDEPORE column and compare its potential to that of other commercially available columns. Preliminary scouting gradients were performed to find out the optimal gradient condition that can be applied for the comparative study. According to the first results, a linear gradient from 30% B to 70% B provided reasonable retention on all columns. During the systematic comparative measurements, the volume fractions of acetonitrile at the beginning and end of the gradient were set constant to 30% and 70%, respectively ($\Delta\phi = 0.40$). Each gradient run was followed by column re-equilibration (at the end of each gradient run, the mobile phase composition was held at 70% B for 0.5 min, then the initial gradient condition was reset and run for 2 min to re-equilibrate the system for the next injection).

For peak capacity measurements, the solvent strength was varied linearly with gradient times ranging from 10 to 110 min (t_g = 10, 30, 50, 70, 90 and 110 min). The peak capacity of each column was investigated at two different chromatographic linear velocities (u = 0.12 and 0.19 cm/s, equivalent to F = 0.25 and 0.40 ml/min, which are commonly used flow rates with 2.1 mm I.D. columns). The columns were thermostated at 50 °C. The injected volume was 1 μL (partial loop with needle overfill mode), and UV detection at 210 nm (20 Hz) was applied (20 Hz data acquisition rate was found to be sufficient since the sharpest peaks eluted with ~4 s baseline peak width). Since all experimental parameters

have been kept constant, these conditions can be used to effectively compare the peak capacity of the six 150 mm long narrow bore columns in gradient separation of proteins. For both linear velocities, six different gradient times t_g were applied to allow a direct comparison of the peak capacity (n_P) and peak capacity per time unit and pressure unit (PPT) of the six columns at different gradient analysis time. A total of 72 experiments were performed, corresponding to two different linear velocities, six different gradient times and six different columns. In gradient elution mode, the samples focus at the inlet of the column, therefore only the contribution of the connecting tube after the column and the detector cell contribute to the peak broadening. This extra-column peak variance in gradient elution mode was found to be negligible.

Peak capacity is a concept first described by Giddings [18] and soon put to good use by Horvath for gradient chromatography [19]. It is a measure of the separation power that includes the entire chromatographic space together with the variability of the peak width over the chromatogram. The general expression for peak capacity (n_c) in liquid chromatography, assuming unit resolution between the successively eluted peaks can be written as [20]:

$$n_c = 1 + \int_{t_I}^{t_F} \frac{1}{4\sigma} dt \tag{4}$$

where t_I is the retention time of the first eluted peak, t_F is the retention time of the last eluted peak, dt is a dummy time variable, and σ is the time standard deviation of a peak. For the practical comparison of different columns in gradient elution mode, several different experimental formulas are often used [21–25]. In this study, peak capacities were experimentally determined from the gradient time (t_g) and the average measured peak width at 50% height ($W_{50\%}$). The following equation was used to estimate the peak capacity based on peak width at 4σ, corresponding to a resolution of $Rs = 1$ between consecutive peaks:

$$n_c = 1 + \frac{t_g}{1.7 \cdot w_{50\%}} \tag{5}$$

In order to avoid the imprecision associated with the measurement of peak widths at base for proteins often containing closely related variants (i.e. for a heterogeneous sample) the peak width at half height was preferred in this study. This way, the impurities present in the sample and partially resolved from the main component did not confuse the measurement.

The peak width of different sized proteins can be significantly different, therefore to present real-life examples, only the peak width of one protein peak was considered for the calculations. It shows the cases of real-life separations when generally the same or very similar molecular weight proteins are separated (e.g. native form, oxidized forms, deamidated forms or reduced forms). Calculations were performed for medium size and large proteins and peak capacity versus gradient time plots were constructed (see Section 3.2).

The column performance also depends on column permeability (K_v) and retention time, the latter being related to column dead time and gradient time. Therefore, peak capacity plots do not give information about the achievable separation time, but only about the reachable peak widths. By analogy to Knox's separation impedance concept [17], similar representation of kinetic performance can be constructed by calculating the peak capacity per unit time and per unit pressure values, according to the next formula [26]:

$$\mathrm{PPT} = \frac{n_c}{t_g \cdot \Delta P} \tag{6}$$

where PPT is the peak capacity per unit time and per unit pressure value, t_g is the gradient run time and ΔP is the column pressure drop. Plots of PPT as a function of gradient steepness (in logarithmic scale) were constructed to compare the "separation impedance" of the different columns when the experimental conditions correspond to different gradient steepness at constant flow rate.

The opposite case, when the flow rate is changed but the gradient steepness is kept constant can be easily presented in gradient kinetic plots. Different gradient kinetic plots have been presented by Wang et al., Zhang et al., Haddad et al. and Ruta et al. but these types of plots were obtained by using a computerized optimization algorithm [27–30]. For constructing the gradient kinetic plots, the recently introduced simple method of the Desmet group was applied [31,32]. The gradient steepness was kept constant during the measurements of gradient van Deemter like curves for the different columns. The steepness was chosen as $\beta t_0 = 3$ which is a good starting point for 150 mm long narrow bore columns (β is the time steepness of the gradient, t_0 is the column dead time). This gradient steepness corresponds for example to a 15 min long gradient at 0.3 ml/min flow rate. The linear velocity was varied from 0.024 up to 0.265 cm/s (u_0 = 0.024, 0.048, 0.072, 0.096, 0.120, 0.144, 0.169, 0.193, 0.217, 0.241 and 0.265 cm/s), while the gradient time was set accordingly (t_g = 90, 45, 30, 22.5, 18, 15, 12.9, 11.3, 10, 9 and 8.2 min, respectively), to achieve similar gradient steepness. The columns were thermostated at 50 °C during these measurements. The column permeability was determined by the following equation:

$$K_v = \frac{u_0 \cdot \eta \cdot L}{\Delta P} \tag{7}$$

where K_v is column permeability, u_0 is velocity of unretained species, L is column length and η is the maximum mobile phase viscosity during the gradient program (η = 0.76 cP). Permeability data were obtained after correction for the system pressure drop. The column dead time (t_0) was calculated as:

$$t_0 = \frac{\Delta P_{\max}}{\eta} \left(\frac{K_v}{u_0^2} \right) \tag{8}$$

where $\Delta P_{\max}$ is related to the column mechanical stability (or instrument limitation in terms of maximum operational pressure). Peak capacity was calculated on the basis of observed gradient plate counts (N_{obs}) and retention time according to the method of Broeckhoven et al. [31]. Then, the t_0 versus peak capacity plots were constructed to compare the achievable analysis time at constant gradient steepness.

3. Results and discussion

3.1. Comparison of the achievable plate heights obtained with narrow bore and standard bore Aeris WIDEPORE columns

The kinetic properties of the columns of two different diameters were evaluated based on Knox plots obtained with estradiol, ivermectin and insulin as test analytes.

The Aeris WIDEPORE packing material is available in both conventional (4.6 mm and 3 mm I.D.) and narrow-bore (2.1 mm I.D.) columns. It is a general observation that the efficiency of the former tends to be markedly higher than that of the latter. It was shown that the landmark performance of columns packed with the Kinetex 2.6 μm particles (another core–shell material) is only limited to the standard bore column (4.6 mm I.D.). However, when packed in a narrow bore format (2.1 mm I.D.), the reduced plate height of 1.8 and 1.9 were the minimum achieved [4,33]. This suggests that the packing of narrow bore columns does not provide comparable packed bed homogeneity to that of the standard bore columns. Gritti and Guiochon studied the mass transfer kinetics of the Kinetex 1.7 μm C18 packed in a 2.1 mm I.D. column, and the minimum reduced plate height above 2.0 was obtained [34]. This provides further suggestion that the problematic situation of packing narrow bore columns is compounded when the packing materials are finer

such as the sub-2 μm particles. According to Gritti and Guiochon, the difference in efficiency is accounted for by the contribution to the column H of the long-range eddy diffusion term which is larger with 2.1 than in the 4.6 mm I.D. columns [35]. While the associated relative velocity biases are of comparable magnitude in both types of columns, the characteristic radial diffusion lengths are of the order of 100 and 40 μm in the wall regions of narrow-bore and conventional columns, respectively [35].

In this study, reduced plate height minimum values of h_{min} = 1.8 and 1.7 were observed with the narrow bore Aeris WIDEPORE column by injecting small analytes (estradiol and ivermectin) (Fig. 1A and B). With the same test analytes, a h_{min} of 1.4 was achieved with the standard 4.6 mm I.D. Aeris WIDEPORE column. These values slightly differ from those previously reported for Kinetex columns (d_p = 2.6 μm, 0.35 μm shell thickness, 100 Å) [4]. Theoretically, the diameter of the solid core and the thickness of the shell or the external diameter of the particle characterizes the chromatographic properties of the packing material, therefore lower reduced plate height minimum is expected with the Aeris WIDEPORE, since the ratio of the radii of the solid core (Ri) to that of the particle (Re) is $\rho = Ri/Re = 1.57/1.80 = 0.87$ while $\rho = 0.73$ for the Kinetex material (the average shell thickness of 0.23 μm for Aeris material was taken from Phenomenex on the basis of personal discussion). According to some recent modelling, a reduced plate height minimum of around or under h_{min} = 1.0 is expected for particles having core–shell structure with $\rho = 0.87$ [36,37]. In practice, the expected efficiency of Aeris WIDEPORE column in isocratic mode (for small analytes) was significantly lower than in theory. However, the narrow bore Aeris WIDEPORE column provided lower reduced plate height minimum values than the Kinetex 2.6 μm or 1.7 μm materials packed into narrow bore columns. It is necessary to mention that this discussion ignores the fact that the two materials are different not only in particle size and particle structure but also in shell morphology and surface roughness.

The performance of Aeris WIDEPORE in protein separations is of more interest since this material was dedicated for the analysis of large molecules. Fig. 1C shows the obtained h–ν plots for insulin. Both the standard and narrow bore Aeris WIDEPORE columns demonstrated impressive reduced plate height values. Even if it is difficult to attain the ν_{opt} value with such a large compound, less than h_{min} = 2.0 reduced plate heights were observed with both the standard and narrow bore Aeris WIDEPORE columns at reduced linear velocities $\nu < 4$ ($u < 0.02$ cm/s). It is noteworthy that at elevated temperature both columns gave significantly better performance. Approximately 20–30% gain in efficiency in the C-term region of the Knox curves was observed when the columns were operated at 50 °C compared to 35 °C, due to improved diffusion at elevated temperature (D_M proportional to the ration T/η).

3.2. Protein separation, peak capacity, the effect of gradient steepness

When it comes to separate high molecular weight compounds, which have low diffusivity, the column performance is mostly determined by the mass transfer resistance. Recent work suggests that the improvement in mass transfer of the current generation of shell particles can be mostly explained by the reduction in external film mass transfer resistance and not by the reduction in transparticle mass transfer resistance [9]. Increasing the shell porosity accessible to proteins accelerates the mass transfer through the stationary film surrounding the shell particles. According to a recent study of Gritti and Guiochon, the external film mass transfer resistance controls more than 90% of the solid–liquid mass transfer resistance of proteins [9]. The external film transfer becomes slower with decreasing access to the internal volume. Therefore, theoretically efficient protein separation requires fine shell type particles having large porosity, large average pore size and decreased shell thickness.

In the following section, a systematic study presents the peak capacity of two columns packed with wide pore conventional fully porous particles, two columns packed with sub-2 μm fully porous particles (175 and 300 Å), one column packed with the new 3.6 μm wide-pore shell particles and one column of 2.7 μm 160 Å shell particles in gradient protein separations. The column dimensions were identical (150 mm × 2.1 mm) and all of them were made with C18 material. This methodical comparison allows us to study the effect of both pore size and particle structure (fully porous or shell type) on the performance in gradient separation mode. In practice, proteins are separated in gradient elution mode at elevated temperature. Elevated temperature is beneficial because it decreases the secondary interactions between residual silanols and positively charged biomolecules. Moreover, the use of high temperatures strongly enhances analyte diffusion [38,39]. Furthermore, ion-pairing reagents such as TFA should be preferentially added to the mobile phase in order to increase the efficiency of protein separation [40–42]. For the reason of emulating real-life separations, we applied 50 °C as column temperature, added 0.1% TFA into the mobile phase and used gradient spans between 10 and 110 min which are fairly common in the current practice. The test solution was a mixture of model proteins (insulin, cytochrome c, myoglobin and BSA) having different molecular weights comprised between 5.7 and 66.8 kDa.

The influence of the gradient steepness and linear velocity on column performance was investigated under several gradient elution conditions. These experimental variables are directly related to the mobile phase flow-rate and the gradient time duration which are often used to adjust a proper separation in practical every day work. The former has a direct influence on the peak width while gradient duration plays an important role on the resolution under gradient conditions as it affects the retention factor of the solute in the mobile phase composition upon elution. The peak capacity of 150 mm long narrow bore Aeris WIDEPORE C18, Ascentis Express Peptide ES C18, Waters BEH300 C18 Hypersil Gold C18, Zorbax 300SB C18 and Jupiter C18 columns were calculated and plotted against the gradient time (t_g = 10–110 min, in 20 min increments) according to Eq. (5) at two different flow rates (F = 0.25 and 0.40 ml/min) (Fig. 2). These results illustrate how significantly the experimental conditions affect the peak capacity of core–shell and fully porous materials as well as demonstrate significant differences in column performance when proteins are separated. It should be stressed that these conditions are not meant to maximize the peak capacity for any particular column or compound as sometimes higher peak capacity can be achieved by choosing longer gradient times. Instead, we merely wanted to identify a set of conditions that allows a fair comparison within a practically acceptable time frame, for the 150 mm long narrow bore columns used in this study. Peak capacity and separation impedance values were calculated and compared based on the peak widths of proteins of different molecular size.

3.2.1. Performance with a small protein (insulin, 5.7 kDa)

The six columns gave very similar peak capacity values for the smallest protein (data not shown). This means that all of the six columns are suitable for the separation of small proteins with sufficient efficiency. Particles with both 160 and 175 Å nominal pore sizes are adequate for the separation of proteins smaller than 6 kDa (approx. 30–35 Å in size, depending on the protein structure). The peak capacity reached n_c = 600 with a 110 min long gradient time on the Acquity BEH300 and Aeris WIDEPORE columns and about $n_c \sim 550$ with the Peptide ES and Jupiter columns. The Hypersil Gold column gave $n_c \sim 500$ while the Zorbax 300SB column performed

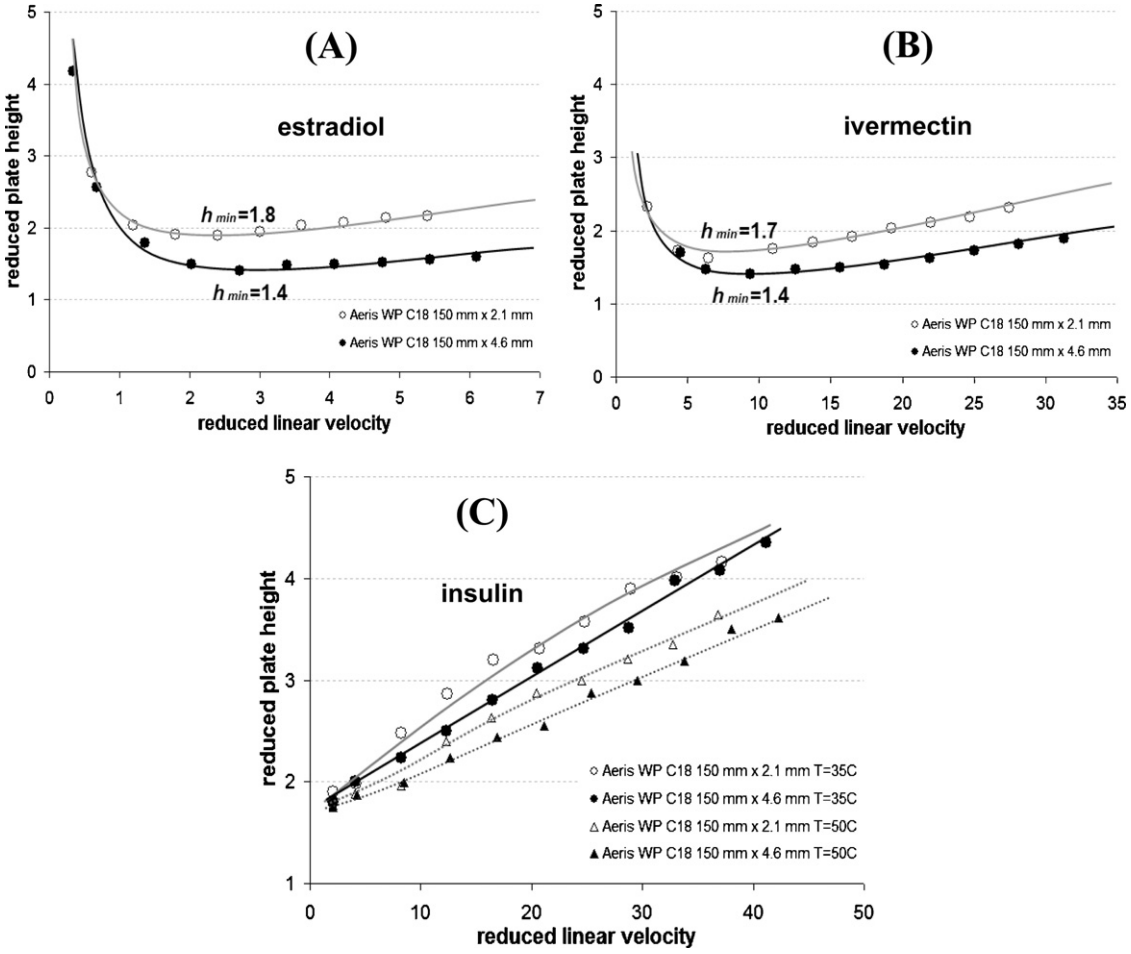

Fig. 1. Reduced plate height versus reduced linear velocity plots of 3.6 μm core–shell type (Aeris WIDEPORE) column. Experiments were conducted on 150 mm long narrow bore (2.1 mm) and standard bore (4.6 mm) columns. Test analytes: estradiol (A), ivermectin (B) and insulin (C). Estradiol was eluted with acetonitrile/water 20/80 (v/v), ivermectin was eluted with acetonitrile/water 75/25 (v/v), and insulin was eluted with acetonitrile (0.1% TFA)/water (0.1% TFA) 30/70 (v/v). The temperature was set to 35 °C in the case of estradiol and ivermectin and both 35 °C and 50 °C for insulin. Injected volume: 0.5 μL.

$n_c \sim 460$. The maximum of the peak capacity was not reached even with a 110 min long gradient time.

3.2.2. Performance with a moderate size protein (myoglobin, 17.7 kDa)

Fig. 2A shows the obtained peak capacity as a function of gradient time with myoglobin as test protein at a relatively low flow rate (0.25 ml/min). The fully porous 175 Å sub-2 μm packing (Hypersil Gold) seems to be inappropriate for the separation of such a large protein (17.7 kDa). A maximum peak capacity of $n_c \sim 200$ was reached with the 110 min long gradient. The column packed with particles having similar pore size but shell structure (Peptide ES) provided significantly better peak capacity for this protein. In spite of the fact that the manufacturer of this column states that this material is suitable only for small proteins (molecular weights below 15 kDa), this column performs approximately 1.8 times better in term of peak capacity compared to the column packed with similar pore sized fully porous very fine particles. Obviously, the shell structure is a benefit in protein separations although some recent results suggest that the intraparticle mass transfer is not as a significant contributor to the total mass transfer process, as previously thought [9]. According to this study, the external film mass transfer is supposed to be the dominant contributor to the total mass transfer. This contribution is dependent on the particle diameter. According to the theory, approximately the same efficiency could be expected with these 2.7 μm shell type and 1.9 μm fully porous material, if the access of the molecules to the pore is unrestricted. Probably the explanation of this different behaviour lies in different pore structure (such as pore size distribution) of the two materials. Further work is in progress to characterize and compare the six packing materials investigated in this study with respect to their pore size distribution, particle size distribution and total porosity in order to better interpret these observations.

The 3.6 μm wide-pore shell type column and the 300 Å fully porous 1.7 μm column provide very similar peak capacities in the case of the 17.7 kDa protein. This observation is in agreement with theoretical expectations. By applying a 90 min long gradient $n_c = 438$ and $n_c = 458$ were achieved with the Aeris WIDEPORE and Acquity BEH300 columns, respectively, which was very impressive for such a large protein. It is interesting that the peak capacity did not reach its maximum with the Acquity wide pore column even with a 110 min long gradient while the Aeris WIDEPORE column reached its maximum performance at 70–75 min gradient time ($n_{c,max} = 445$, it corresponds to a gradient steepness of $\beta = 0.53\%$ B/min). If we consider that the column permeability of the Aeris WIDEPORE (3.6 μm) is significantly higher than that of a column packed with sub-2 μm material, and since this column generates very similar peak capacity, it is easy to conclude that considerably faster separations can be achieved with the Aeris WIDEPORE than with the Acquity BEH300 column.

With the conventional 5 μm material (Zorbax), a maximum peak capacity of $n_c \sim 260$ was reached with the 110 min long

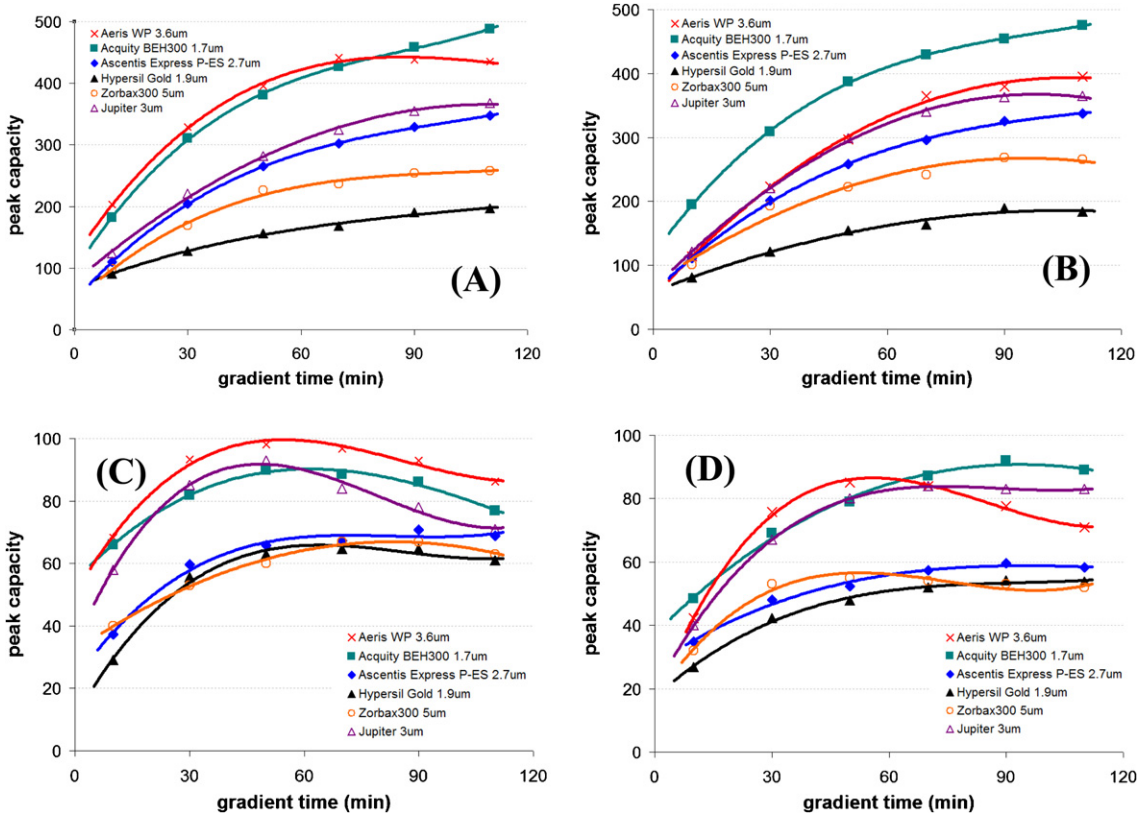

Fig. 2. Peak capacity plots of Myoglobin at 0.25 ml/min (A) and at 0.40 ml/min (B) flow rate, and of BSA at 0.25 ml/min (C) and at 0.40 ml/min (D) flow rate. Columns: Aeris WIDEPORE C18 (150 mm × 2.1 mm), Acquity BEH300 C18 (150 mm × 2.1 mm), Ascentis Express Peptide ES C18 (150 mm × 2.1 mm), Hypersil Gold C18 (150 mm × 2.1 mm), Zorbax 300SB C18 (150 mm × 2.1 mm) and Jupiter C18 (150 mm × 2.0 mm). Temperature: 50 °C, injected volume: 1 μL, detection: 210 nm. Mobile phase A: 0.1% TFA in water, mobile phase B: 0.1% TFA in acetonitrile. Gradient: from 30% to 70% B with varying gradient times.

gradient while the 3 μm wide pore conventional column (i.e. Jupiter) provided significantly higher peak capacity ($n_c \sim 370$). In this comparison the Jupiter 3 μm fully porous and the shell type Peptide ES columns have shown very similar performance.

Fig. 3A shows the peak capacity per pressure and time unit (PPT) values as a function of the gradient steepness. In this type of presentation, the higher the PPT value, the lower the "separation impedance" is. These plots illustrate that the fastest separation can be achieved with the Aeris WIDEPORE column. However, the Aeris WIDEPORE reached its limitation in terms of peak capacity (Fig. 2A), therefore whenever a separation requires very high peak capacity values ($n_c > 445$) the Acquity BEH300 column should be a better option. The "separation impedance" of Zorbax and Jupiter columns is practically identical and noteworthy in this type of comparison, because of their high permeability. The Ascentis Express Peptide ES and Acquity BEH300 columns provides similar separation impedance, while the Hypersil Gold column presents the highest "separation impedance" in this comparison because of its low permeability and poor peak capacity with large biomolecules.

When the flow rate was elevated to 0.4 ml/min, the Acquity BEH300 column significantly outperforms the other columns based on peak capacity only (Fig. 2B). There was a remarkable loss in peak capacity at 0.4 ml/min compared to 0.25 ml/min in the case of Aeris WIDEPORE column of about 25%, while this decrease was only 5% with the Hypersil Gold column and it was nearly negligible with the Acquity BEH300, Ascentis Express Peptide ES, Zorbax 300SB and Jupiter columns. The significant efficiency loss of Aeris WIDEPORE column can be probably explained with its relatively large particle size ($d_p = 3.6$ μm), since the optimum in linear velocity and the contribution of the mass transfer resistance to the total H is a function of particle diameter. Possibly 0.4 ml/min was far above the optimum mobile phase velocity with this particle size. At 0.4 ml/min the Acquity BEH300 column gives 20% higher peak capacity than the Aeris WIDEPORE column for the moderate size protein myoglobin. If the column permeability is considered too, the Aeris WIDEPORE column still offers the chance of the fastest separation (Fig. 3B) if the required peak capacity was $n_c < 380$ (Fig. 2B).

3.2.3. *Performance with a large protein (BSA, 66.8 kDa)*

The efficient separation of large proteins is always a great challenge. Large proteins are typically not homogeneous, may adopt numerous different conformations (possibly related to microheterogeneity which manifest itself as various isoforms), and undergo posttranslational modifications. This extensive sample complexity can manifest itself in chromatography in the form of broadened peaks. Moreover, the unrestricted access of such large proteins to pores is always an additional issue.

Fig. 2C shows the peak capacity plots of BSA obtained at 0.25 ml/min flow rate. In this case, the new Aeris WIDEPORE column outperforms all the other columns. The latter provides 10–15% and 7–20% higher peak capacity than the Acquity BEH300 and Jupiter, respectively. The kinetic performance of Ascentis Express Peptide ES, Hypersil Gold and Zorbax columns was very similar in this comparison. These three columns gave approximately half the peak capacity of the Aeris WIDEPORE column. In case of the Peptide ES and Hypersil Gold columns, exclusion of this large molecule from pores is highly probable since the average pore size is only 160 Å and 175 Å, respectively. All of the tested columns reached their maximum performance within the investigated gradient span range. The PPT plots of BSA demonstrate that in case of large proteins such as BSA, the Aeris WIDEPORE column should

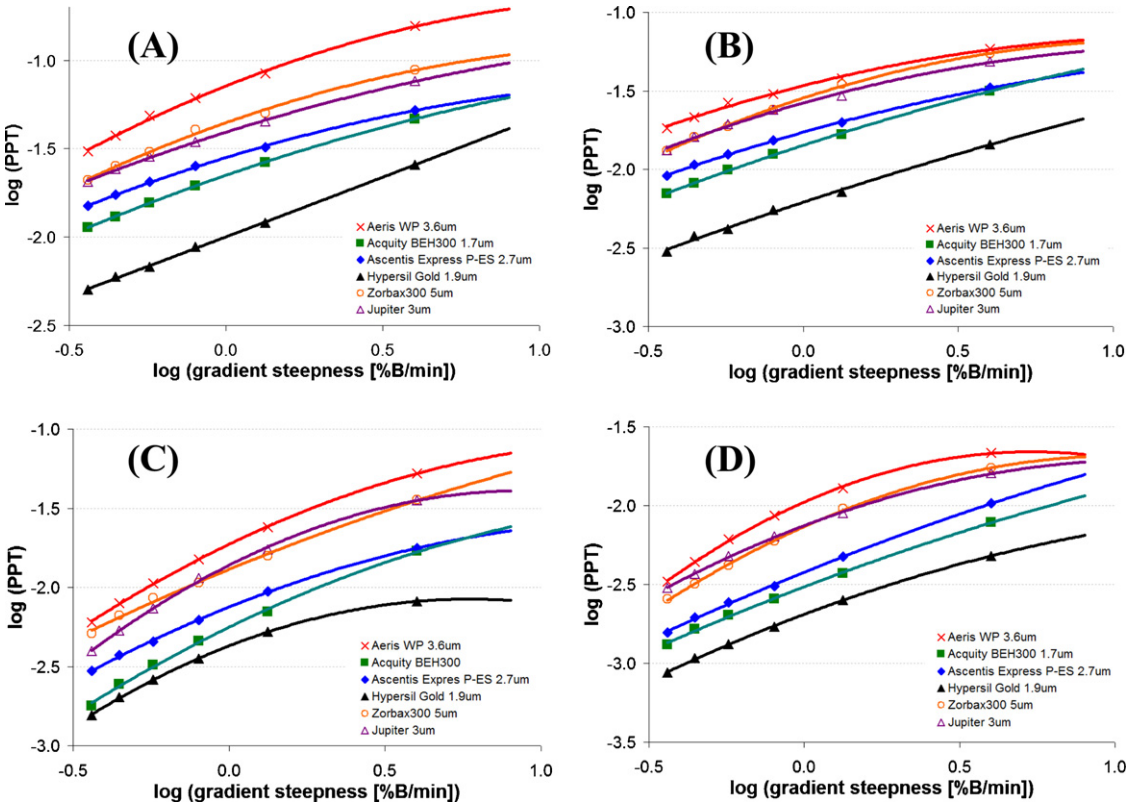

Fig. 3. Gradient separation impedance (peak capacity per time unit and per pressure unit versus gradient steepness) plots of Myoglobin at 0.25 ml/min (A) and at 0.40 ml/min (B) flow rate, and of BSA at 0.25 ml/min (C) and at 0.40 ml/min (D) flow rate. Experimental conditions as specified in Fig. 2.

provide the fastest separation (Fig. 3C). The advantage of the Aeris WIDEPORE column was more significant for large protein separations. Fig. 4 shows the chromatograms of BSA obtained on the Aeris WIDEPORE, Acquity BEH300 and Ascentis Express Peptide ES columns at the flow rate of 0.25 ml/min. Obviously the Aeris WIDEPORE column produces the most symmetrical and the sharpest peak.

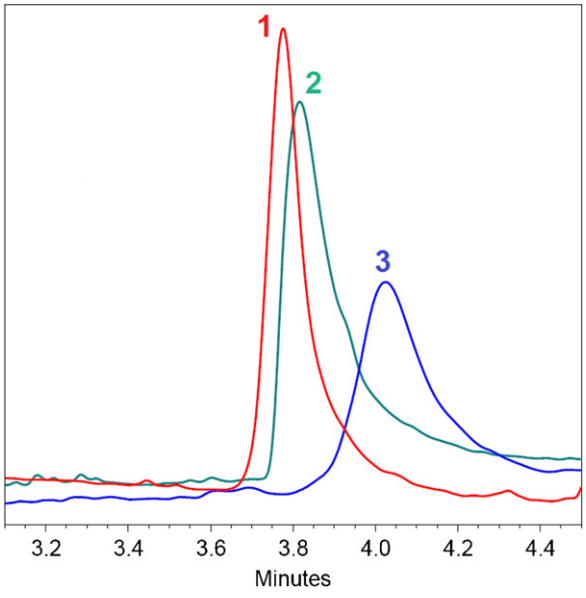

Fig. 4. Zoomed chromatograms of BSA. Columns: (1) Aeris WIDEPORE C18 (150 mm × 2.1 mm), (2) Acquity BEH300 C18 (150 mm × 2.1 mm), and (3) Ascentis Express Peptide ES C18 (150 mm × 2.1 mm). Temperature: 50 °C, injected volume: 1 μL, detection: 210 nm. Mobile phase A: 0.1% TFA in water, mobile phase B: 0.1% TFA in acetonitrile. Gradient steepness: $\beta = 4\%\Delta B/\text{min}$.

As the flow rate was increased to 0.4 ml/min, the Aeris WIDEPORE, Ascentis Express Peptide ES and Hypersil Gold column lose approximately 20% peak capacity compared to 0.25 ml/min. The loss in peak capacity was around 10–15% with the conventional columns (Zorbax and Jupiter) while the observed efficiency loss with the Acquity BEH300 column was only around 2–3% (Fig. 2D). Both the Acquity and Jupiter columns outperform the Aeris WIDEPORE when long, flat gradients were used ($\beta < 0.5$, or gradient time was longer than 65 min in this case). But, when the separation speed was also important, the use of Aeris WIDEPORE column was still more beneficial. It can be seen in Fig. 3D that the Aeris WIDEPORE column gives higher PPT values than all the other columns.

It is noteworthy that the maximum peak capacity values dropped drastically for all columns (60–85% loss) in case of the BSA compared to myoglobin. With the applied conditions, when gradient steepness was varied between $\beta = 0.36$ and 4.00, the observed maximum peak capacity of BSA was only around $n_c \sim 90$–100 (for the Aeris WIDEPORE, Acquity BEH300 and Jupiter 150 mm long columns).

As a conclusion, we can state that the Aeris WIDEPORE column is very advantageous for the separation of large proteins. Faster separations can be achieved with the Aeris compared to the other columns. However, it is necessary to note that the Aeris WIDEPORE column losses its efficiency – as the mobile phase velocity is increased – more drastically than columns packed with conventional fully porous, sub-3 or sub-2 μm particles such as the Zorbax, Jupiter, Acquity BEH300 or Peptide ES column. For this reason, it would be interesting to have an Aeris WIDEPORE material with a lower particle size than 3.6 μm.

3.3. Protein separations, gradient kinetic plots and the effect of flow rate

The effect of mobile phase flow rate on the peak capacity was studied in more detail by means of gradient kinetic plots [27–32]. With the help of gradient kinetic plots it is easy to map the peak width against mobile phase flow rate at constant gradient steepness. In our study, a general gradient steepness was chosen at $\beta t_0 = 3$. The kinetic performance of columns was mapped by measuring the observed plate counts at 11 different flow rates (and the corresponding gradient times). These experiments allow to compare the achievable maximum separation speed on the different columns taking into account both their permeability and mechanical stability (maximum allowable operational pressure). However, this strategy can be applied only for one value of the gradient steepness at a time, which is the limitation of this approach.

In this work, a mixture of model proteins including insulin, cytochrome c and BSA was injected. Three different gradient kinetic plots were constructed on the basis of the observed peak width of the three different proteins. In this way it is possible to evaluate the column efficiency for different cases, when small (insulin), medium size (cytochrome c) or large proteins (BSA) have to be separated.

Fig. 5 shows the obtained gradient kinetic plots of t_0 versus peak capacity. The permeability of the compared columns was assessed from the experimental column pressure (ΔP).

The plots in Fig. 5A show that the peak capacity produced by the six tested columns was reasonably similar in the case of a small protein such as insulin (as the curves lie very close to each other). However, in the range of low peak capacity values ($n_c < 250$) the separation was faster with the Aeris WIDEPORE column, while for separations requiring high peak capacity ($n_c > 250$) the Ascentis Express Peptide ES column offers the fastest separation. As an example, if we want to have a peak capacity of $n_c = 200$ and if we assume a gradient retention of $k_e = 5$, the separation will take 29 min with the Aeris WIDEPORE, 33 min with the Ascentis Express Peptide ES, 40 min with the Acquity BEH300, 50 min with the Hypersil Gold and approximately 65 min with the Jupiter and Zorbax columns.

It is necessary to mention that the mechanical stability of the column has an important consequence on the minimum achievable separation time. Nominally, the Aeris WIDEPORE column is stable up to 600 bar while the Acquity BEH300 is stable up to 1000 bar. The BEH300 column generates approximately 4-times higher back pressure than the Aeris WIDEPORE column, it has only 1.7 times higher mechanical stability than the Aeris WIDEPORE one. Therefore, when equivalent peak widths were generated by the two columns, the Aeris WIDEPORE could achieve a 2.4-times faster separation, if the maximum performance was utilized.

In the case of medium size proteins such as cytochrome c, the importance of pore size becomes more critical. In this case, the 300 Å Acquity and Aeris WIDEPORE materials clearly outperform the medium pore (175 Å and 160 Å) and conventional wide pore columns (Fig. 5B). In the peak capacity range of $n_c = 60–150$, the Acquity BEH300 and Aeris WIDEPORE columns provide equivalent efficiency, but when the separation demands high peak capacity, the use of Aeris WIDEPORE column is more practical since it offers significantly shorter analysis time at its maximal operating pressure.

In the case of large proteins such as BSA (Fig. 5C), the difference in column performance was more evident. All of the investigated columns generated relatively low kinetic performance. By applying this particular gradient steepness, only $n_c = 40–100$ can be achieved. The Aeris WIDEPORE column provides the highest peak capacity and the shortest analysis whenever the separation requires peak capacities of $n_c > 30$. However, whenever fast separation is desired (in the range of high flow rates), the Acquity BEH300 column outperforms the Aeris WIDEPORE column. This probably can be explained by the relatively large particle size of Aeris WIDEPORE ($d_p = 3.6$ μm). Most likely the optimum linear velocity is considerably higher in the case of the 1.7 μm Acquity BEH300 material than it is with the 3.6 μm Aeris WIDEPORE. Another observation is that the 175 Å fully porous sub-2 μm porous material is evidently not suitable for the separation of large proteins. The columns packed with 2.7 μm shell particles having similar nominal pore size (160 Å), can provide 5–8 times faster separations than the fully porous 1.9 μm material. Therefore, the shell structure plays an important role in the mass transfer of large proteins and seems to be exceptionally advantageous. Surprisingly, the conventional wide pore 3 μm Jupiter column offers similar analysis time as the Acquity column. The performance of 5 μm wide pore packing (Zorbax 300SB) was also very close to the performance of Ascentis Express Peptide ES column in this comparison.

3.4. Real-life examples

3.4.1. Separation of closely related proteins

Characterization of a biological product, conducted by appropriate analytical techniques, provides information on efficiency of expression and efficacy of purification procedures [43]. According to European Pharmacopoeia (Ph.Eur.) monograph for filgrastim concentrated solution, product related impurities are divided into following groups: (a) impurities with molecular masses higher than that of filgrastim; (b) impurities with molecular masses differing from that of filgrastim; (c) impurities with charges differing from that of filgrastim; and (d) other filgrastim related proteins [44]. Filgrastim is used to treat neutropenia (low neutrophils blood count), by stimulating the bone marrow to increase production of neutrophils. Causes of neutropenia include chemotherapy and bone marrow transplantation. The pharmacopoeia suggests a 60 min long reversed-phase separation for quantifying the oxidized forms of the filgrastim. Several other reversed-phase methods can be found in the literature on the separation of these oxidized forms [45,46].

In this section, the kinetic performance of the six columns was compared in terms of their peak capacity when a fast gradient separation was used to separate filgrastim related proteins. The chromatographic conditions were optimized by a systematic variation of the gradient span and steepness, and of the column temperature and flow rate. It was found that a fast 6.5 min long gradient was appropriate to separate the filgrastim related oxidized and reduced proteins on all six 150 mm long narrow bore columns. Actually, the Hypersil Gold and Zorbax SB300 columns failed to separate the four oxidized forms. In these conditions, the Aeris WIDEPORE column provided the highest peak capacity ($n_c = 114$). The peak capacity obtained with Acquity BEH300 was comparable ($n_c = 103$) while the Peptide ES, Jupiter, Zorbax 300SB and Hypersil Gold columns provided significantly lower efficiency ($n_c = 87$, 76, 72 and 50, respectively). Fig. 6 shows the representative chromatograms of filgrastim related proteins obtained with the Aeris WIDEPORE and Acquity BEH300 columns. Since filgrastim is a popular recombinant biosimilar product (also commercialized under the brand names Neupogen, Graffel, Religrast, Nugraf, Shylgrast, Neukine, Emgrast, Amoytop filgrastim), this method can be applied in the bio-pharmaceutical industry in the long-term stability testing for the analysis of product related protein impurities or degradants. The advantage of this method was the short analysis time and its very high separation power compared to the other RP-HPLC methods reported in the literature.

3.4.2. Separation of monoclonal antibody fragments

The use of RP-HPLC as an analytical tool for monitoring intact monoclonal antibodies (mAbs) has been limited because

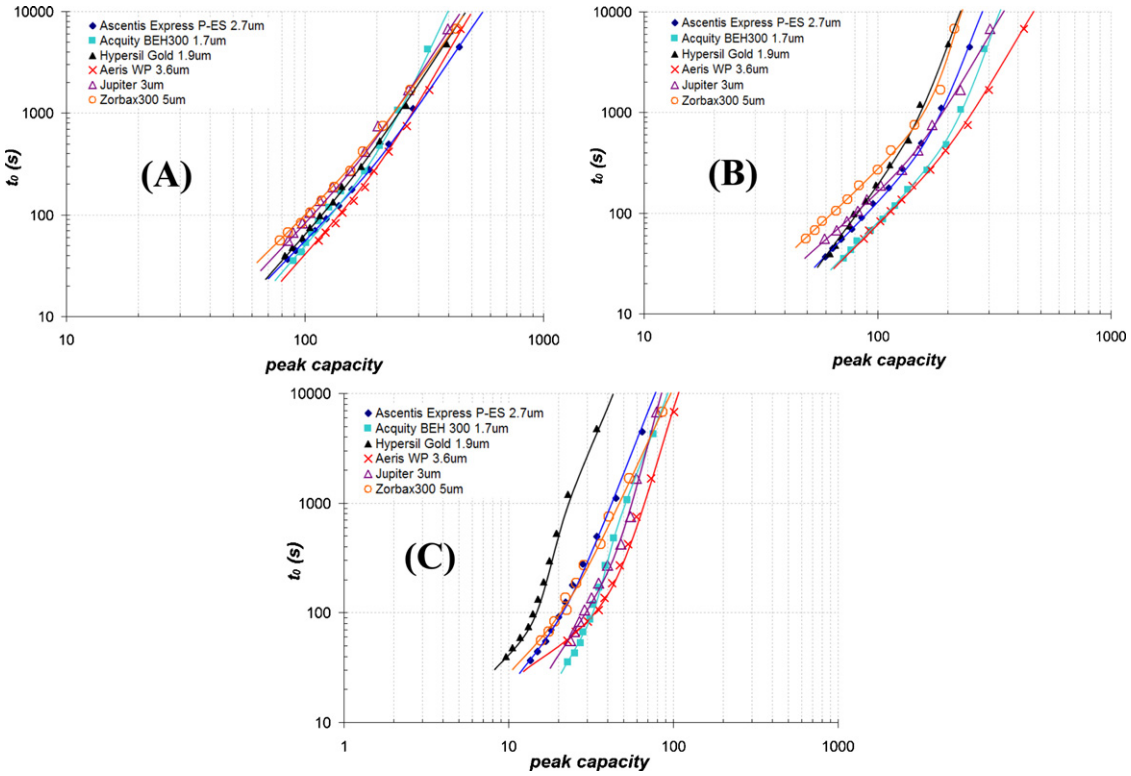

Fig. 5. Gradient kinetic plots of insulin (A), cytochrome C (B) and BSA (C). Columns: Aeris WIDEPORE C18 (150 mm × 2.1 mm, max pressure drop: 600 bar), Acquity BEH300 C18 (150 mm × 2.1 mm, max pressure drop: 1000 bar), Ascentis Express Peptide ES C18 (150 mm × 2.1 mm, max pressure drop: 600 bar), Hypersil Gold C18 (150 mm × 2.1 mm, max pressure drop: 1000 bar), Zorbax 300SB C18 (150 mm × 2.1 mm, max pressure drop: 400 bar) and Jupiter C18 (150 mm × 2.0 mm, max pressure drop: 400 bar). Temperature: 50 °C, injected volume: 1 μL, detection: 210 nm. Mobile phase A: 0.1% TFA in water, mobile phase B: 0.1% TFA in acetonitrile. Maximum viscosity of mobile phase $\eta = 0.76$ cP. Gradient: from 30% to 70% B, gradient steepness $\beta t_0 = 3$.

of the complex and hydrophobic nature of these very large macromolecules [47]. However, efforts in developing reversed-phase method for antibody characterization recently demonstrated acceptable recovery, peak shape and minimal column interactions for several IgG1 antibodies [48]. In addition, antibodies display intrinsic heterogeneity with respect to glycosylation, fragmentation, oxidation, deamidation, pyroglutamate, truncation, and disulfide shuffling [49–52]. Therefore, there is a need to improve the chromatographic analysis of these antibodies and to resolve the variants and degradants associated with antibody heterogeneity and stability. In this section, the performance of the new Aeris WIDEPORE column is presented in monoclonal antibody separation.

In many cases, antibody heterogeneity is related to conformational isoforms of equivalent molecular weight. The reduction of the disulfide bonds and then, the subsequent RP-HPLC separation of the resulted fragments is a commonly used test to determine whether the conformational variants are disulfide-related or not [47]. The IgG antibody was reduced with DTT and chromatographic conditions were optimized to resolve as many variants as possible

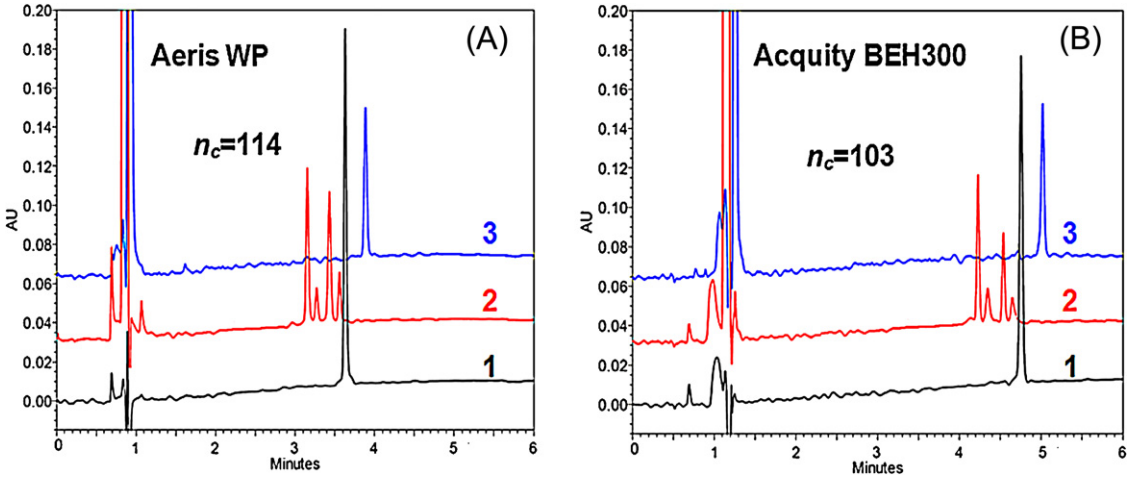

Fig. 6. Comparative chromatograms of filgrastim related proteins obtained with Aeris WIDEPORE and Acquity BEH300 150 mm × 2.1 mm columns. Chromatogram 1: native filgrastim, chromatogram 2: oxidized forms, chromatogram 3: reduced form. Conditions: Mobile phase A: 0.1% TFA in water, mobile phase B: 0.1% TFA in acetonitrile, flow rate: 300 μL/min, gradient: 45–65% B in 6.5 min, temp: 80 °C, injected volume: 2 μL, detection at 210 nm.

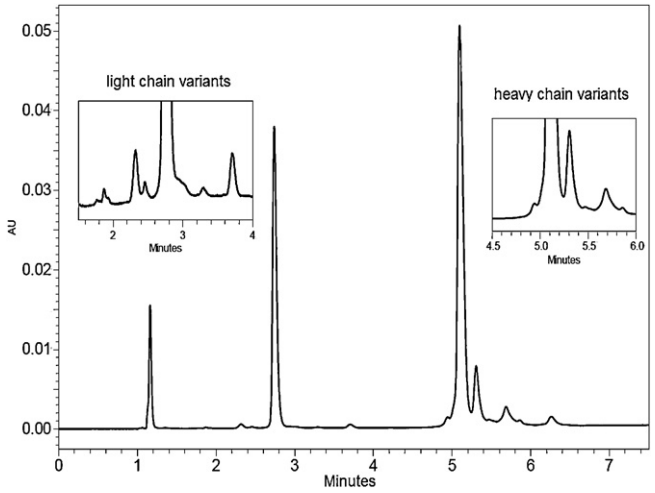

Fig. 7. Representative chromatogram of reduced IgG monoclonal antibody (50 and 25 kDa fragments). Conditions: Mobile phase A: 0.1% TFA in water, mobile phase B: 0.1% TFA in acetonitrile, flow rate: 250 μL/min, gradient: 30–37% B in 8 min, temp: 75 °C, injected volume: 0.5 μL, detection at 280 nm, column: AERIS WIDEPORE 150 mm × 2.1 mm, 3.6 μm.

within reasonable analysis time. A relatively steep (0.88% B/min), fast gradient (8 min) at elevated temperature (75 °C) provided an efficient separation of the antibody fragments. The obtained chromatogram of the resulted light chain (LC) and heavy chain (HC) fragments is presented in Fig. 7. The separation power of the Aeris WIDEPORE column allows us to observe several variants of both the LC and HC.

Another typical method in antibody analysis is papain digestion. Papain cleaves IgG antibodies into three fragments (two Fab fragments and one Fc fragment). Generally, ion exchange chromatographic methods are used to resolve the Fab and Fc variants. In this example, the Fab and Fc fragments were reduced to generate smaller (10–25 kDa) fragments. Reversed-phase conditions were optimized, and we conclude that this type of RP-HPLC fragment mapping can be a useful tool in the pharmaceutical industry and can be applied for comparability studies in the field of biosimilar product development. Fig. 8 shows a representative chromatogram of RP-HPLC antibody fragment mapping by using the new Aeris WIDEPORE column. An 8 min long steep gradient (1% B/min) at elevated temperature (75 °C) can separate several variants of the antibody fragments.

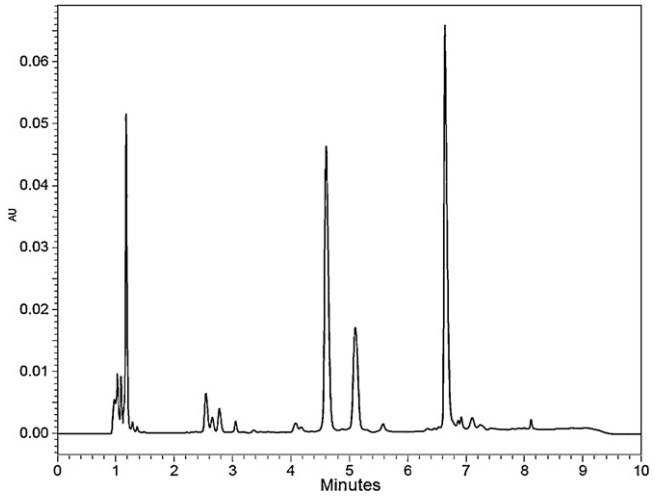

Fig. 8. Representative chromatogram of IgG monoclonal antibody fragment map (10 and 25 kDa fragments). Conditions: Mobile phase A: 0.1% TFA in water, mobile phase B: 0.1% TFA in acetonitrile, flow rate: 250 μL/min, gradient: 28–36% B in 8 min, temp: 75 °C, injected volume: 0.5 μL, detection at 280 nm, column: AERIS WIDEPORE 150 mm × 2.1 mm, 3.6 μm.

4. Conclusion

In this study, the new wide-pore core–shell material recently released by Phenomenex under the trademark Aeris WIDEPORE was evaluated. This material possesses an average particle size of 3.6 μm, a porous layer of ~0.2 μm (the porous layer represents only 34% of the total particle volume) and pores large enough to be suitable for protein analysis. This new chromatographic support was evaluated using some usual chromatographic figures of merit in the isocratic (h_{min}) and gradient elution modes (peak capacity and peak capacity per time and pressure units). Its performance was compared with those of the Waters Acquity BEH300 C18 1.7 μm porous particles, Hypersil GOLD C18 175 Å 1.9 μm porous particles, Ascentis Express Peptide ES C18 160 Å 2.7 μm shell particles and conventional wide pore Zorbax SB300 5 μm as well as Jupiter 3 μm fully porous particles.

First of all, some small model drugs (MW < 1000 Da) were selected and the h_{min} values of 2.1 and 4.6 mm I.D. Aeris WIDEPORE columns were determined. The values were equal to 1.4 and 1.7–1.8 for the 4.6 and 2.1 mm I.D. columns, respectively. These values are close to those often reported in the literature for shell particles. The 4.6 mm I.D. columns are always presenting a better packing quality. The achievable lowest h values were also determined for insulin (5.7 kDa) at 35 and 50 °C. More surprisingly, the observed values were below 2 whatever the column I.D. and temperature. This demonstrates the potential of the Aeris WIDEPORE material for protein separations.

Since real-life separations of proteins are always performed in the gradient elution mode, the performance of the six different 150 mm narrow bore columns was evaluated under such conditions using the model proteins, insulin, cytochrome c, myoglobin and BSA, with molecular weights comprised between 5.7 and 66.8 kDa. In a first instance, the peak capacities were calculated at two different flow rates, 0.25 and 0.4 ml/min for various gradient times between 10 and 110 min. It appears that the Aeris WIDEPORE and Acquity materials showed higher separation power than the other columns for large proteins but provided similar efficiency for small proteins such as insulin. It has to be noted that the Peptide ES and Hypersil Gold columns were not designed for medium/large protein analysis. At elevated flow rates or with long gradient times, the Acquity material often outperformed the other columns. However, due to the very low backpressure generated by the 3.6 μm core–shell particles, the Aeris WIDEPORE material surpasses the other columns based on peak capacity per time and pressure unit, whatever the mobile phase flow rate and gradient steepness. Additionally, the effect of mobile phase flow rate on peak capacity was studied in more detail by means of the gradient kinetic plot methodology. The behaviour of the six columns was found to be very similar for the small protein insulin (5.7 kDa) while the difference between columns becomes more and more evident when increasing the size of the model proteins. Finally, for the two largest proteins, namely cytochrome c (12.4 kDa) and BSA (66.8 kDa); the Acquity BEH300, Aeris WIDEPORE and Jupiter materials proved to be significantly better than the other stationary phases.

The different columns were also evaluated for the separation of real-life samples of filgrastim (18.8 kDa) and its oxidized and reduced forms. As expected, the performance of the six columns could be ranked in the following order: Aeris WIDEPORE > Acquity BEH300 > Peptide ES > Jupiter > Zorbax 300SB > Hypersil Gold, for this separation. This confirms the theoretical investigations initially performed. The Aeris WIDEPORE material was also tested for

the analysis of reduced as well as digested mAb. Some impressive separations in less than 7 and 10 min were, respectively, attained.

Finally, this column packed with 3.6 μm particles can be compatible with a conventional HPLC instrumentation in terms of pressure providing that extra-column and system dwell volumes are minimized or if a last generation of HPLC instrument is considered. In addition, because of the reasonable backpressure generated, a preparative column would be interesting to purify complex protein samples with high throughput.

Acknowledgements

The authors wish to thank Dr Tivadar Farkas (Phenomenex Inc) for providing the Aeris WIDEPORE columns. Harald Ritchie and Thierry Domenger From Thermo Fisher scientific are also acknowledged for the gift of Thermo Hypersil Gold 150 mm × 2.1 mm, 1.9 μm column.

References

[1] J.J. DeStefano, T.J. Langlois, J.J. Kirkland, J. Chromatogr. Sci. 46 (2008) 254.
[2] J.M. Cunliffe, T.D. Maloney, J. Sep. Sci. 30 (2007) 3104.
[3] S. Fekete, J. Fekete, K. Ganzler, J. Pharm. Biomed. Anal. 49 (2009) 64.
[4] E. Oláh, S. Fekete, J. Fekete, K. Ganzler, J. Chromatogr. A 1217 (2010) 3642.
[5] S. Fekete, K. Ganzler, J. Fekete, J. Pharm. Biomed. Anal. 54 (2011) 482.
[6] G. Guiochon, F. Gritti, J. Chromatogr. A 1218 (2011) 1915.
[7] S. Fekete, E. Oláh, J. Fekete, J. Chromatogr. A 1228 (2012) 57–71.
[8] S.A. Schuster, B.M. Wagner, B.E. Boyes, J.J. Kirkland, J. Chromatogr. Sci. 48 (2010) 566.
[9] F. Gritti, G. Guiochon, J. Chromatogr. A 1218 (2011) 907.
[10] S.A. Schuster, B.E. Boyes, B.M. Wagner, J.J. Kirkland, J. Chromatogr. A 1228 (2012) 232–241.
[11] A. Staub, D. Zurlino, S. Rudaz, J.L. Veuthey, D. Guillarme, J. Chromatogr. A 1218 (2011) 8903–8914.
[12] S. Fekete, J. Fekete, J. Chromatogr. A 1218 (2011) 5286.
[13] D.S. Smyth, S. Utsumi, Nature 216 (1967) 334.
[14] J.W. Goding, Monoclonal Antibodies: Principles and Practice, Academic Press, Florida, FL, 1983, p. 118.
[15] K.G. Moorhouse, W. Nashabeh, J. Deveney, N.S. Bjork, M.G. Mulkerrin, T. Ryskamp, J. Pharm. Biomed. Anal. 16 (1997) 593.
[16] P.A. Bristow, J.H. Knox, Chromatographia 10 (1977) 279.
[17] C.R. Wilke, P. Chang, AIChE J. (1955) 264.
[18] J.C. Giddings, Anal. Chem. 39 (1967) 1027.
[19] Cs. Horvath, S.R. Lipsky, Anal. Chem. 39 (1967) 1893.
[20] U.D. Neue, J. Chromatogr. A 1079 (2005) 153.
[21] X. Wang, D.R. Stoll, A.P. Schellinger, P.W. Carr, Anal. Chem. 78 (2006) 3406.
[22] J.W. Dolan, L.R. Snyder, N.M. Djordjevic, D.W. Hill, T.J. Waeghe, J. Chromatogr. A 857 (1999) 1.
[23] U.D. Neue, J.R. Mazzeo, J. Sep. Sci. 24 (2001) 921.
[24] U.D. Neue, J.L. Carmody, Y.-F. Cheng, Z. Lu, C.H. Phoebe, T.E. Wheat, Adv. Chromatogr. 41 (2001) 93.
[25] U.D. Neue, Y.-F. Cheng, Z. Lu, in: S. Kromidas (Ed.), HPLC Made to Measure: A Practical Handbook for Optimization, Wiley-VCH, Weinheim, 2006, p. 47.
[26] X. Wang, W.E. Barber, P.W. Carr, J. Chromatogr. A 1107 (2006) 139.
[27] X. Wang, D.R. Stoll, P.W. Carr, P.J. Schoenmakers, J. Chromatogr. A 1125 (2006) 177.
[28] Y. Zhang, X. Wang, P. Mukherjee, P. Petersson, J. Chromatogr. A 1216 (2009) 4597.
[29] T.J. Causon, E.F. Hilder, R.A. Shellie, P.R. Haddad, J. Chromatogr. A 1217 (2010) 5063.
[30] J. Ruta, D. Guillarme, S. Rudaz, J.L. Veuthey, J. Sep. Sci. 33 (2010) 2465.
[31] K. Broeckhoven, D. Cabooter, F. Lynen, P. Sandra, G. Desmet, J. Chromatogr. A 1217 (2010) 2787.
[32] K. Broeckhoven, D. Cabooter, S. Eeltink, G. Desmet, J. Chromatogr. A 1228 (2012) 20–30.
[33] J. Ruta, D. Zurlino, C. Grivel, S. Heinisch, J.L. Veuthey, D. Guillarme, J. Chromatogr. A 1228 (2012) 221–231.
[34] F. Gritti, G. Guiochon, J. Chromatogr. A 1217 (2010) 5069.
[35] F. Gritti, G. Guiochon, J. Chromatogr. A 1218 (2011) 1592.
[36] K. Kaczmarski, G. Guiochon, Anal. Chem. 79 (2007) 4648.
[37] J. Kostka, F. Gritti, K. Kaczmarski, G. Guiochon, J. Chromatogr. A 1218 (2011) 5449.
[38] H. Chen, Cs Horvath, J. Chromatogr. A 705 (1995) 3.
[39] S. Heinisch, J.L. Rocca, J. Chromatogr. A 1216 (2009) 642.
[40] R.A. Everley, T.R. Croley, J. Chromatogr. A 1192 (2008) 239.
[41] A. Shibue, C.T. Mant, R.S. Hodges, J. Chromatogr. A 1080 (2005) 58.
[42] A. Shibue, C.T. Mant, R.S. Hodges, J. Chromatogr. A 1080 (2005) 68.
[43] L.S.A. Vanz, G. Renard, S.M. Palma, M.J. Chies, S.L. Dalmora, L.A. Basso, S.D. Santos, Microbiol. Cell Fact. 7 (2008) 1.
[44] European Pharmacopoeia 6.3. Filgrastim Concentrated Solution 01/2009:2206, EDQM.
[45] A. Skrlina, E.K. Krnica, D. Gosaka, B. Prestera, V. Mrsab, M. Vuletica, D. Runaca, J. Pharm. Biomed. Anal. 53 (2010) 262.
[46] R. Pavisic, K. Hock, I. Mijic, A. Horvatic, M. Gecan, M. Sedic, M.B. Krajacic, M. Cindric, Int. J. Pharm. 387 (2010) 110.
[47] T.M. Dillon, P.V. Bondarenko, D.S. Rehder, G.D. Pipes, G.R. Kleemann, M.S. Ricci, J. Chromatogr. A 1120 (2006) 112.
[48] T.M. Dillon, P.V. Bondarenko, M.S. Ricci, J. Chromatogr. A 1053 (2004) 299.
[49] A. Beck, M.C. Bussat, N. Zorn, V. Robillard, C. Klinguer-Hamour, S. Chenu, L. Goetsch, N. Corvaia, A. Van Dorsselaer, J.F. Haeuw, J. Chromatogr. B 819 (2005) 203.
[50] A.J. Chirino, A. Mire-Sluis, Nat. Biotechnol. 22 (2004) 1383.
[51] T.M. Dillon, M. Speed Ricci, D. Rehder, G. Pipes, Y. Zhang, N. Stackhouse, A. Huinker, M.J. Treuheit, P.V. Bondarenko, Proceedings of the 52th ASMS Conference, Nashville, Tennessee, 2004, WPD065, A042883 (CD).
[52] D. Rehder, T.M. Dillon, P.V. Bondarenko, Proceedings of the 52th ASMS Conference, Nashville, Tennessee, 2004, MPU393, A042863 (CD).